Electrochimica Acta 54 (2009) 4844–4850

Contents lists available at ScienceDirect

Electrochimica Acta

journal homepage: www.elsevier.com/locate/electacta

Investigation of carbon-supported Pt and PtCo catalysts for oxygen reduction in direct methanol fuel cells

S. Siracusano [a], A. Stassi [a], V. Baglio [a,1], A.S. Aricò [a,1], F. Capitanio [b], A.C. Tavares [b,*,1]

[a] CNR-ITAE, Via Salita Santa Lucia Sopra Contesse 5, 98126 Messina, Italy
[b] Institut National de la Recherche Scientifique-Énergie, Matériaux et Télécommunications, 1650 Boulevard Lionel Boulet, Varennes, Québec, Canada, J3X 1S2

ARTICLE INFO

Article history:
Received 15 January 2009
Received in revised form 26 March 2009
Accepted 28 March 2009
Available online 7 April 2009

Keywords:
Direct methanol fuel cells
Oxygen reduction
Methanol tolerance
Polarizations
ac-impedance spectroscopy
Cyclic voltammetry

ABSTRACT

Carbon-supported Pt and Pt_3Co catalysts with a mean crystallite size of 2.5 nm were prepared by a colloidal procedure followed by a carbothermal reduction. The catalysts with same particle size were investigated for the oxygen reduction in a direct methanol fuel cell (DMFC) to ascertain the effect of composition. The electrochemical investigations were carried out in a temperature range from 40 to 80 °C and the methanol concentration feed was varied in the range 1–10 mol dm^{-3} to evaluate the cathode performance in the presence of different conditions of methanol crossover. Despite the good performance of the Pt_3Co catalyst for the oxygen reduction, it appeared less performing than the Pt catalyst of the same particle size for the cathodic process in the presence of significant methanol crossover. Cyclic voltammetry analysis indicated that the Pt_3Co catalyst has a lower overpotential for methanol oxidation than the Pt catalyst, and thus a lower methanol tolerance. Electrochemical impedance spectroscopy (EIS) analysis showed that the charge transfer resistance for the oxygen reduction reaction dominated the overall DMFC response in the presence of high methanol concentrations fed to the anode. This effect was more significant for the Pt_3Co/KB catalyst, confirming the lower methanol tolerance of this catalyst compared to Pt/KB. Such properties were interpreted as the result of the enhanced metallic character of Pt in the Pt_3Co catalyst due to an intra-alloy electron transfer from Co to Pt, and to the adsorption of oxygen species on the more electropositive element (Co) that promotes methanol oxidation according to the bifunctional theory.

1. Introduction

Portable power sources are one of the most promising applications of direct methanol fuel cells (DMFCs) [1]. Methanol is a liquid fuel, easy to handle, with very high specific energy density (~6 kWh/kg), and DMFCs have intrinsically higher energy density and improved autonomy than batteries. In addition, DMFCs have the potential for instantaneous re-charge (refuelling). High energy density requires the utilization of high concentration of methanol so the size of the fuel reservoir in the DMFC can be reduced [2]. However, the fuel cell operation with concentrated methanol is seriously limited by the permeation of methanol across the polymer electrolyte membrane (methanol crossover) which results in a significant loss in the fuel and voltage efficiencies. Current DMFCs operating at low temperature use high loadings of Pt catalyst in the cathode to enhance the oxygen reduction reaction (ORR) in the presence of methanol crossover. The methanol adsorbs on the Pt sites at the cathode, and a mixed potential, resulting from the oxygen reduction and methanol oxidation occurring simultaneously, reduces the cell voltage [1].

One approach to circumvent this problem is to develop novel Pt-based catalysts capable of enhancing the oxygen reduction reaction but with limited activity, or even inert, for methanol oxidation. Pt-based alloy catalysts, such as Pt-M (M = Fe, Ni, Co, Cr, Cu) have been proposed and tested as methanol tolerant cathode catalysts for DMFCs based on the following: (i) the second metal could block the methanol adsorption on Pt due to a dilution effect [3–10] since the dissociative adsorption of methanol requires the existence of several adjacent Pt ensembles [1,11], and (ii) binary Pt-based alloy catalysts exhibit an enhanced electrocatalytic activity for the ORR in comparison with Pt alone [12–15] due to the increased Pt d-band vacancy (electronic factor) [16] and by a favourable Pt–Pt interatomic distance (geometric effect) [17].

There is a vast literature on methanol tolerant Pt-M alloy cathode catalysts for DMFCs and it has been recently reviewed by Antolini et al. [7,18]. There is some disagreement in the literature over the improvement of methanol tolerance and DMFC performance through the formation of Pt-M alloy catalysts [1,7,19], and the reasons could be in the different alloys compositions, or in the use of different synthetic methods resulting in different degrees of alloying, surface composition and particle size. The large majority

* Corresponding author. Tel.: +1 450 929 8947; fax: +1 450 929 8102.
E-mail address: tavares@emt.inrs.ca (A.C. Tavares).
[1] ISE member.

0013-4686/$ – see front matter © 2009 Elsevier Ltd. All rights reserved.
doi:10.1016/j.electacta.2009.03.070

of the DMFC studies on bimetallic catalysts for ORR were carried out with diluted methanol at the anode (1–2 mol dm^{-3}, except for one case where the authors went up to 4 mol dm^{-3} [4]), with pressurized oxygen feed at a cathode and at temperatures higher than 60 °C. Although some of these experimental conditions are more favourable for the ORR, they are often far from those envisaged for portable applications. Finally, it is difficult to draw conclusions about the effect of the second metal on the methanol tolerance of a Pt catalyst when both composition and particle size in the catalytic systems are different.

The aims of the present work were: (i) to evaluate the performance of a state of the art Pt-Co catalyst for PEFC fuel cells [12] in DMFCs operating at low temperature and with concentrated methanol, and (ii) to try to clarify the effect of the second metal (Co) in the alloy on the methanol tolerance of Pt cathode catalyst. For this purpose a Pt-Co alloy catalyst characterized by a high concentration of metallic phase (50 wt.%) on carbon black (Ketjenblack) and an optimum mean crystallite size for the ORR [20] was synthesised using the carbothermal reduction method. A 50 wt.% Pt on Ketjenblack catalyst with the identical particle size was also prepared using the same method and used for comparison. Gas diffusion electrodes with Pt loading of 3 mg cm^{-2} were fabricated using the two catalysts, assembled with Nafion 117 membrane and a PtRu anode, and tested in a DMFC. Under such circumstances, any difference in the methanol tolerance or DMFC performance can be directly ascribed to the cathode composition effect.

2. Experimental

2.1. Catalysts preparation

A 50 wt.% Pt/Ketjenblack (Pt/KB) was synthesised through the sulfite-complex route [20,21]. For this purpose, chloroplatinic acid (Engelhard) was used to prepare the $Na_6Pt(SO_3)_4$ precursor. Chloroplatinic acid was dissolved in distilled water and the pH of the solution was adjusted to 7 by adding Na_2CO_3 (Aldrich). Subsequently, $NaHSO_3$ (Aldrich) was added to the solution to obtain a white precipitate of $Na_6Pt(SO_3)_4$, which was filtered, washed copiously with hot distilled water, and dried in an oven at 80 °C. Ketjenblack EC carbon black (BET area 850 m^2/g) was suspended in distilled water and agitated in an ultrasonic water bath at about 80 °C to form a slurry. The appropriate amount of $Na_6Pt(SO_3)_4$ was successively added to the slurry. The Pt sulfite complex was decomposed by adding drop wise a 40% H_2O_2 solution (Carlo Erba) at a temperature of 80 °C, which resulted in vigorous gas evolution. A colloidal PtO_x/KB was obtained in this way. The metallic Platinum supported on carbon (50 wt.% Pt/KB) was finally obtained by carbothermal reduction in inert (Ar) atmosphere at 600 °C. A 50 wt.% Pt-Co/Ketjenblack catalyst with a Pt_3Co atomic composition (Pt_3Co/KB) was prepared using the same colloidal PtO_x/KB followed by impregnation with cobalt nitrate [12,22,23]. After the cobalt precursor impregnation step, a high temperature carbothermal reduction at 600 °C in inert (Ar) atmosphere was used to obtain the carbon-supported PtCo alloy [12]. The resulting catalyst was pre-leached in perchloric acid (0.5 mol dm^{-3}) at 85 °C to remove the non-alloyed cobalt [24].

2.2. Catalysts characterization

X-ray fluorescence (XRF) analysis was used to determine the Pt/Co atomic ratio for the Pt_3Co/KB catalyst. The XRF analysis was carried out by a Bruker AXS S4 Explorer spectrometer operating at a power of 1 kW and equipped with a Rh X-ray source, a LiF 220 crystal analyzer and a 0.12° divergence collimator. The structural characterization of the Pt/KB and Pt_3Co/KB catalysts was done by recording the powder X-ray diffraction (XRD) patterns on a Philips X-pert 3710 X-ray diffractometer using Cu Kα radiation operating at 40 kV and 30 mA. The peak profile of the (2 2 0) reflection in the face centered cubic structure was obtained by using the Marquardt algorithm and used to calculate the crystallite size by using the Debye–Sherrer equation. The morphological characterization was carried out by transmission electron microscopy (TEM) analysis using a FEI CM12 microscope.

2.3. Electrodes fabrication and characterization

2.3.1. DMFC

The in-house prepared Pt/KB or Pt_3Co/KB catalysts were mixed with 15 wt.% Nafion ionomer (Ion Power, 5 wt.% solution) and deposited by a doctor blade technique onto an LT-ELAT gas-diffusion layer (E-TEK, USA). For the anode a commercial unsupported Pt-Ru (1:1 atomic ratio) catalyst (Johnson-Matthey) was mixed with 15 wt.% Nafion ionomer (Ion Power, 5 wt.% solution) and deposited by a doctor blade technique onto the HT-ELAT gas-diffusion layer (E-TEK, USA). The Pt loading was 3 mg cm^{-2} on both anode and cathode. Nafion 117 (Ion Power) was used as electrolyte membrane. Membrane-electrode assemblies (MEAs) were formed by a hot-pressing procedure [25] and subsequently installed in a fuel cell test fixture of 5 cm^2 active area (Fuel Cell Technologies). This latter was connected to a fuel cell test station (model 850C from Scribner Associates) equipped with a FRA unit. The single cells were equilibrated with the humidified gases at room temperature, and for each MEA two cycles of galvanostatic polarizations were recorded between 25 and 80 °C with 1 mol dm^{-3} of aqueous methanol solution fed to the anode chamber of the DMFC through a peristaltic pump (Gilson); humidified air, pre-heated at the same temperature of the cell, was fed to the cathode. Atmospheric pressure in the anode and cathode compartments was used for all experiments. Reactant flow rates were 2 ml min^{-1} and 350 ml min^{-1} for methanol and air stream, respectively. The MEAs performance improved during the first 2 days of operation up to reach a steady-state behaviour. Only the data-set recorded under steady-state conditions is presented.

Galvanostatic polarization curves and short-term stability tests (ca. 2 h) were also recorded for different methanol concentrations (1, 2, 5 and 10 mol dm^{-3}) at 40 °C. Electrochemical impedance spectroscopy (EIS) measurements were carried out as a function of the methanol concentration and were used to evaluate differences in the series and charge transfer resistances between the two MEAs; additional EIS measurements were done with lower and higher air flow rate (220 and 420 ml min^{-1}) and with pure oxygen fed at the cathode (81 ml min^{-1} to keep the same oxygen stoichiometry with respect to air at 350 ml min^{-1}). EIS spectra were recorded in the potentiostatic mode, applying a sinusoidal signal with an amplitude of 10 mV and a frequency in the 10 kHz to 10 mHz range.

2.4. Half cell characterization

For these studies another series of electrodes were prepared as described above but the catalyst inks were applied directly onto carbon cloth substrate (Ballard 1071 HCB) to investigate methanol oxidation under flooded electrode conditions. The Pt loading was 3 mg cm^{-2} for both electrodes.

The half cell characterization was performed in a conventional three-electrode cell (Metrohm) with a platinum wire as counter electrode and a Ag/AgCl reference electrode. All experiments were carried out at room temperature. The electrochemical cell was connected to an Autolab PGSTAT30 Potentiostat/Galvanostat equipped with FRA2 module for impedance spectroscopy. The Pt/KB and Pt_3Co/KB electrodes were characterized by means of cyclic voltammetry (CV) in H_2SO_4 0.5 mol dm^{-3} saturated with nitrogen (high

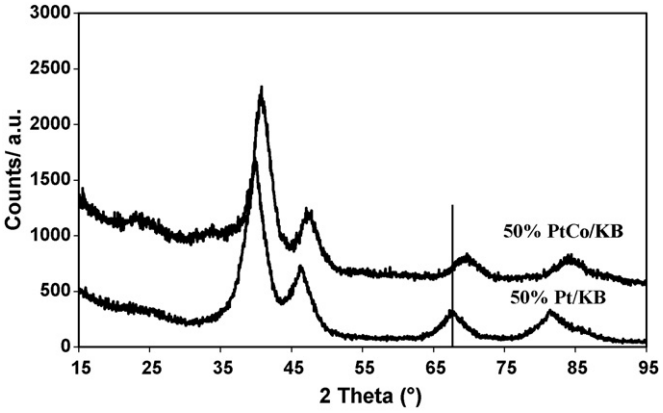

Fig. 1. X-ray diffractograms of Pt/KB and Pt_3Co/KB catalysts.

purity 5.0), and in the presence of methanol 0.5 mol dm^{-3}. Cyclic voltammograms were recorded at a sweep rate of 20 mV s^{-1}.

3. Results and discussion

3.1. Catalysts characterization

The XRF analysis of the Pt_3Co/KB catalyst confirmed a Pt/Co atomic ratio of 3. Fig. 1 reports the XRD patterns of the Pt/KB and Pt_3Co/KB catalysts. Both diffractograms show the typical face centered cubic (fcc) crystallographic structure of platinum and characteristic of the Pt (75 at.%)–Co (25 at.%) alloys [26–28]; no extra peaks related to other crystalline phases were detected for the Pt_3Co/KB catalyst. Assuming only the presence of a fcc structure the degree of alloying was calculated from the lattice contraction determined by XRD and by using the Vegard's law for the solid solution between these two metals [26,28]. A high degree of alloying was found for the Pt_3Co/KB catalyst, as indicated by the significant shift of the reflection peaks to higher (2θ) values due to the decrease of the lattice parameter (Table 1). This is, however, slightly smaller than that reported in the literature for similar composition and crystallographic structure [8,29]. A good agreement between the Pt/Co atomic ratio determined independently by XRF and XRD methods was found for the in-house prepared PtCo/KB catalyst.

The XRD patterns show broad reflection peaks indicating that both catalysts are formed by fine metal particles. The mean crystallite sizes were determined by line broadening analysis (Table 1). The mean diameters of Pt and Pt_3Co crystallites are 2.6 and 2.5 nm, respectively. The morphology of both Pt/KB and Pt_3Co/KB catalysts was analysed by TEM. As shown in Fig. 2a and b, the two catalysts consist of fine particles with almost identical dimensions, in accordance to the XRD analysis, distributed homogeneously on the carbon support, even for such high metal loading on carbon. Similar particle size and morphology in the catalysts under investigation are important aspects since any difference in the electrochemical activity towards the oxygen reduction and methanol tolerance can be related mainly to the compositional effect. In this work it will be possible to do a straightforward comparison between the compositions of the two catalysts since both have the same particle size.

Table 1
Physicochemical characteristics of Pt/KB and PtCo/KB catalysts.

Catalysts	A220 (nm)	PSD (nm)	Pt/Co ratio (XRD)	Pt/Co ratio (XRF)
50% CoPtKB	0.383	2.5	3.2	3.0
50% PtKB	0.392	2.6	–	–

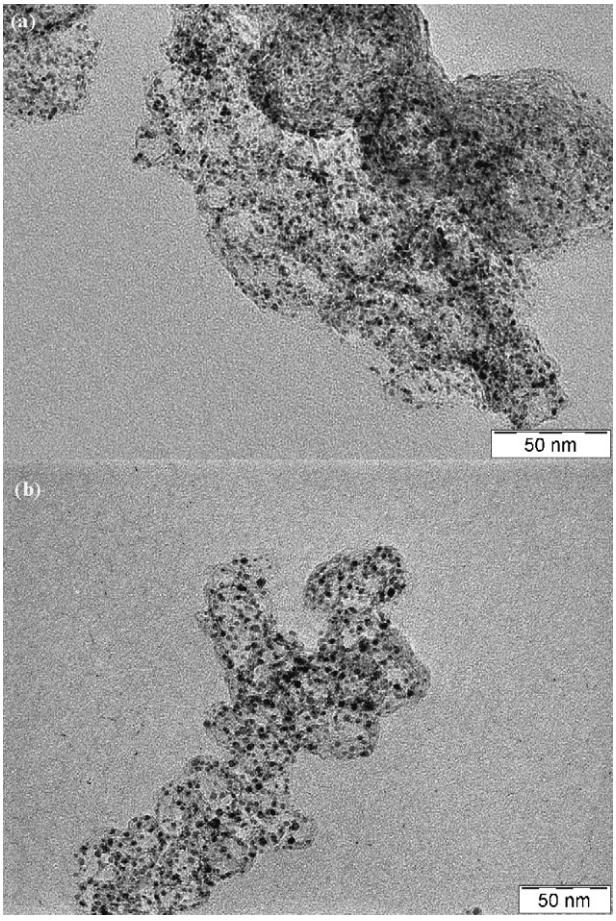

Fig. 2. TEM micrographs of (a) 50% Pt/KB and (b) 50% Pt_3Co/KB catalysts.

3.2. Electrochemical characterization: direct methanol fuel cell

The performance of the Pt/KB and Pt_3Co/KB cathode catalysts was thus investigated in a DMFC with 1 mol dm^{-3} methanol fed at the anode and air fed at the cathode. Fig. 3a compares the polarization behaviour of two single cells equipped with the Pt/KB and Pt_3Co/KB cathode catalysts at 40 and 80 °C. At 40 °C and at low current density (in the activation region) the Pt_3Co/KB catalyst performs better than the Pt/KB catalyst, as expected from the enhanced catalytic activity for ORR of this alloy catalyst with respect to platinum [12,14,29]. The overall performance of both fuel cells is similar within the experimental error (ca. 27 mW cm^{-2}). At 80 °C and low current density the Pt_3Co/KB catalyst appears to show a higher activity for ORR than Pt/KB, whereas the overall performance of the fuel cell with Pt/KB catalyst is superior (45.0 mW cm^{-2} for Pt_3Co/KB and 56.4 mW cm^{-2} for Pt/KB). Since both fuel cells have the same anode and membrane, and since both catalysts have the same morphology and particle size, all variations between the polarization curves can be attributed to differences in the chemical composition between the two oxygen reduction catalysts. The rate of methanol crossover increases with the fuel cell operating temperature [1], and a lower methanol tolerance of Pt_3Co/KB catalyst with respect to Pt/KB catalyst could be the possible cause for the distinct behaviour observed with increasing temperature.

In order to investigate this hypothesis, additional polarization curves were recorded at 40 °C for various methanol concentrations, and up to 10 mol dm^{-3} of methanol. The results are reported in Fig. 4a–c for 2, 5 and 10 mol dm^{-3} methanol solutions. In the activation region the Pt_3Co/KB catalyst performs better for 1–5 mol dm^{-3} methanol concentrations, but for 10 mol dm^{-3} the two catalysts

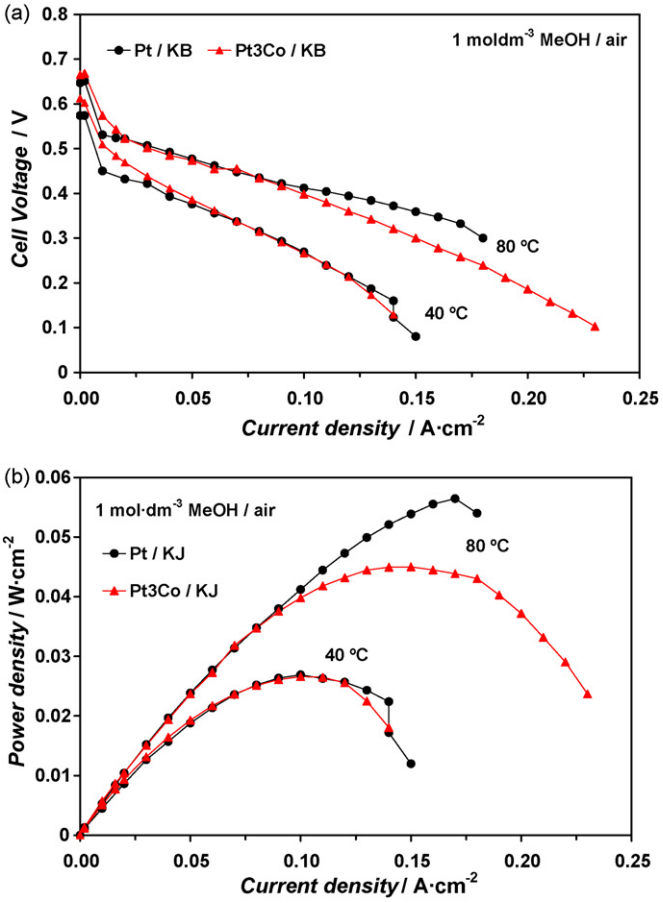

Fig. 3. (a) Polarization and (b) power density curves of single DMFCs with Pt/KB and Pt_3Co/KB cathode catalysts; measurements done at 40 and 80 °C, with 1 mol dm^{-3} MeOH solution and air (atmospheric pressure).

have similar performance. This could be due to a higher catalytic activity for ORR of the alloy catalyst compared to bare Pt, although the methanol tolerance characteristics have also to be taken into account, in particular at high methanol concentration. However, at high current densities the performance of the fuel cell equipped with the Pt/KB catalyst is superior as indicated by the higher cell voltage and lower slope in the *E*–*j* plots. A similar result was observed by Baglio et al. [23] with a DMFC equipped with a Pt-Co/Vulcan XC-72 alloy catalyst operating at 60 °C and with 1 mol dm^{-3} methanol solution.

Fig. 5 reports on the variation of the open circuit voltages and maximum power densities with the methanol concentration. The open circuit voltage (OCV) of the DMFC equipped with the Pt_3Co/KB catalyst is always higher with respect to the values recorded for the Pt/KB based cell confirming the enhanced activity for the ORR of the alloy catalyst. The OCV decreases as a function of methanol concentration due to the increase of methanol crossover. The maximum power density of the DMFC equipped with the Pt_3Co/KB catalyst decreases monotonically with the methanol concentration from 27.6 to 11.6 mW cm^{-2}. For the DMFC equipped with the Pt/KB cathode catalyst the maximum power density is significantly higher in the 2–10 mol dm^{-3} methanol concentration range, and reaches a maximum value of ca. 31 mW cm^{-2} with 2 and 5 mol dm^{-3} methanol solutions. The results shown in Figs. 4 and 5 seem to support our hypothesis on the lower methanol tolerance of the Pt_3Co/KB catalyst with respect to the Pt/KB catalyst.

Both methanol fuel cells were subjected to short-term stability tests at 40 °C. The cell voltage was set to 0.3 V and tests were run with 1, 2, 5 and 10 mol dm^{-3} methanol solutions at the anode and

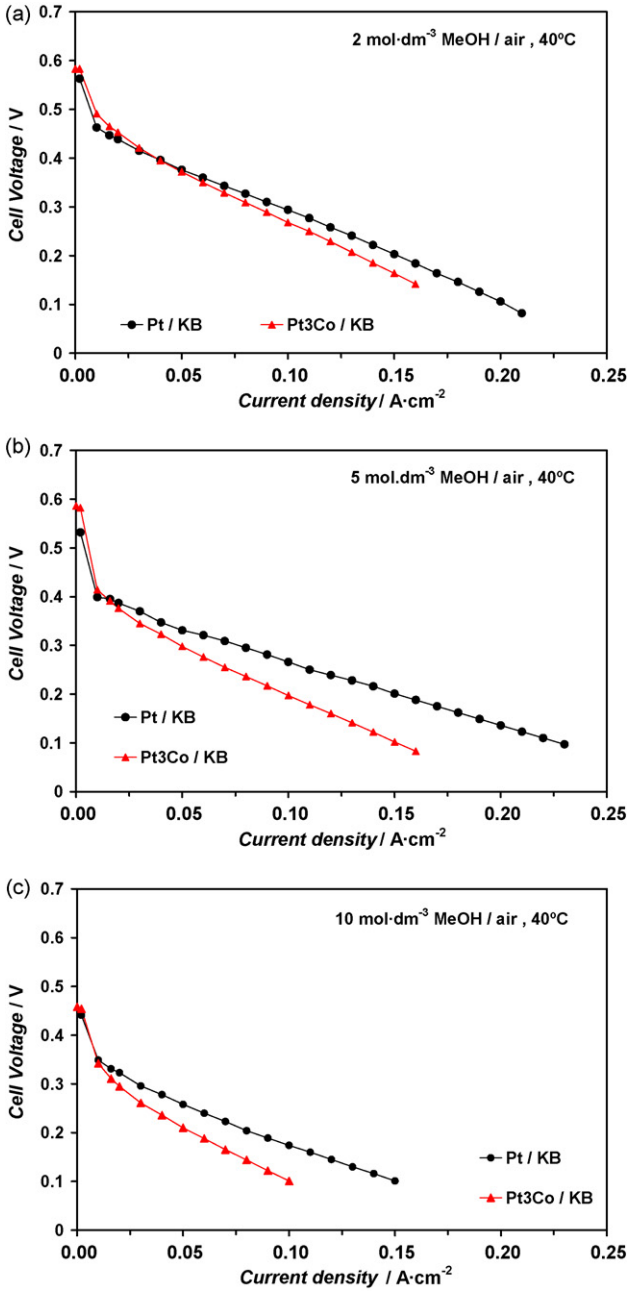

Fig. 4. Polarization curves of single DMFCs with Pt/KB and Pt_3Co/KB cathode catalysts recorded at 40 °C, with air (atmospheric pressure) and different methanol concentrations (a) 2 mol dm^{-3}, (b) 5 mol dm^{-3} and (c) 10 mol dm^{-3}.

air at the cathode. Fig. 6a shows the current density–time profiles recorded for the DMFC equipped with the Pt_3Co/KB catalyst, and Fig. 6b compares the current density values recorded at 100 min as a function of the methanol concentration and cathode catalyst type. The chrono-amperograms of the fuel cell with Pt/KB cathode catalysts are equivalent to those reported in Fig. 6a and therefore not shown. For both DMFCs, the current density decreases slightly for 1 and 2 mol dm^{-3} methanol solutions, while it increases slightly for 5 and 10 mol dm^{-3} methanol solutions.

It is hypothesized that, in the presence of low methanol concentration in the anode feed, the cathode is negatively affected by the continuous methanol permeation through the membrane during operation. The oxidation of methanol permeated through the membrane produces a mixed potential at the cathode. In the presence of large methanol concentration, the elevated methanol crossover

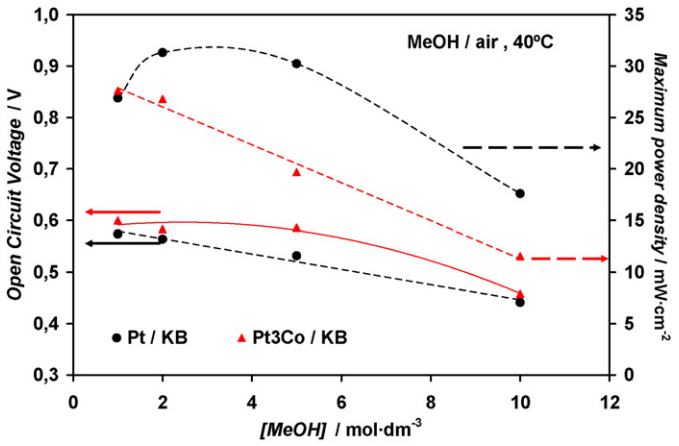

Fig. 5. Open circuit voltage and maximum power density recorded for two single DMFCs with Pt/KB and Pt_3Co/KB cathode catalysts in function of the methanol concentration.

causes the occurrence of large oxidation current at the cathode; this counteracts the oxygen reduction process producing a further lowering of the cathode potential. Thus, the performance decreases significantly when the methanol concentration is increased from 1–2 to 10 mol dm^{-3}. The comparison between the current density values recorded at 100 min confirms what found previously: the performance of both DMFCs in 1 mol dm^{-3} methanol is practically identical, but the DMFC equipped with Pt/KB catalyst performs better in more concentrated methanol (higher methanol tolerance of this catalyst) than the DMFC equipped with the Pt_3Co/KB catalyst.

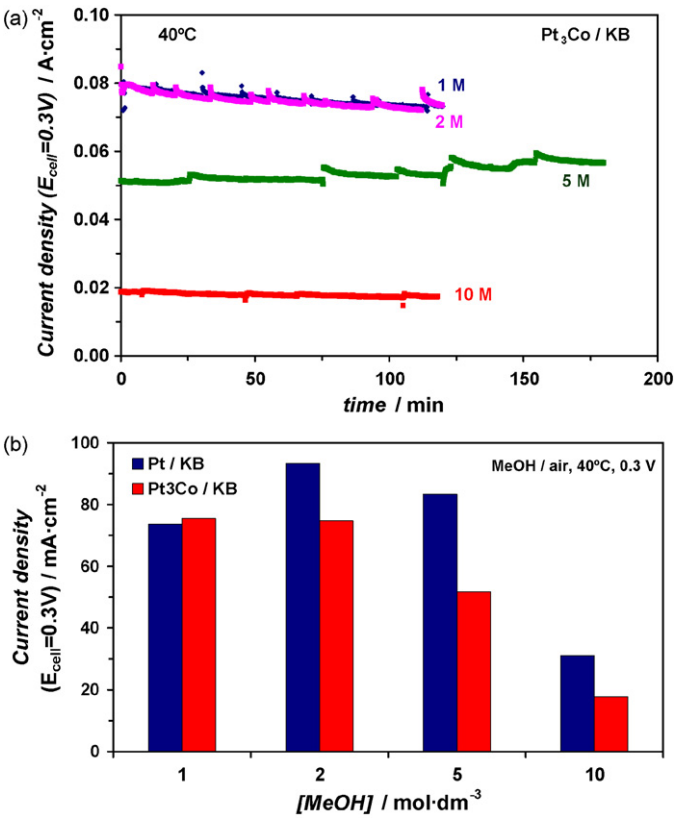

Fig. 6. (a) Chrono-amperometric experiments carried out with the DMFC equipped with the Pt_3Co/KB catalyst for various methanol concentrations (1, 2, 5, 10 mol dm^{-3}); (b) current density recorded after 100 min in function of the methanol concentration and cathode catalyst type; the cell voltage (E_{cell}) was 0.3 V, all experiments were performed at 40 °C and air (atmospheric pressure) was used for the cathode.

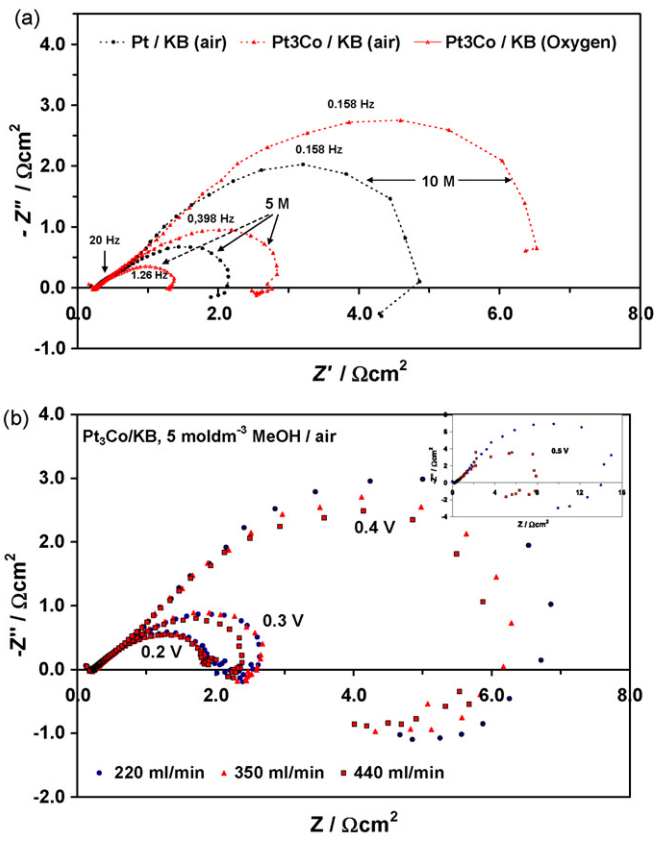

Fig. 7. (a) Nyquist plots of two single DMFCs equipped with the Pt/KB and Pt_3Co/KB cathode catalysts under a cell voltage E_{cell} = 0.3 V, with 5 and 10 mol dm^{-3} methanol solutions and with air or oxygen (atmospheric pressure) and at 40 °C; (b) Nyquist plots of the single DMFCs equipped with the Pt_3Co/KB cathode catalysts in function of the cell voltage and air flow (atmospheric pressure), and with 5 mol dm^{-3} methanol solutions at 40 °C; the dashed lines are just a guide line for the readers and a few frequencies are indicated in a qualitative way.

The maximum performance for the fuel cell equipped with the Pt/KB catalyst is in the 2 and 5 mol dm^{-3} methanol concentration range.

The polarization studies were complemented with EIS analysis and cyclic voltammetry to investigate more in-depth the catalysts' behaviour. The impedance of the two single DMFC cells was measured as a function of the methanol concentration with both air and oxygen feed. Fig. 7a shows the typical impedance spectra of the two DMFCs recorded at a cell potential of 0.3 V, under different conditions of methanol concentration (5 and 10 mol dm^{-3}) and cathode feed (air and pure oxygen).

The series resistance (R_S) measured with the different methanol concentrations and varying the cathode fed was similar for both DMFCs. The total DMFC impedance spectra profiles result from the overlapping of two distorted semicircles. The high frequency semicircle occurs in the 10 kHz to 10 Hz frequency range and the low frequency semicircle occurs in the 10 Hz to 10 mHz frequency range. The amplitude of the second semicircle at low frequency is always larger in the Pt_3Co/KB based cell (Fig. 7a). Since both DMFCs are identical except for the cathode catalyst, it can be concluded that the low frequency arc is related to the cathode. As shown in Fig. 7a, the amplitude of the low frequency arc decreased significantly when the cell impedance was recorded with pure oxygen. The impedance spectrum of a DMFC cathode includes the contribution of the charge transfer impedance of ORR at higher frequency, oxygen diffusion at low frequency and methanol crossover through the inductive loop at very low frequency [30–32]. Additional tests performed under different cell voltages demonstrated that the amplitude of the low

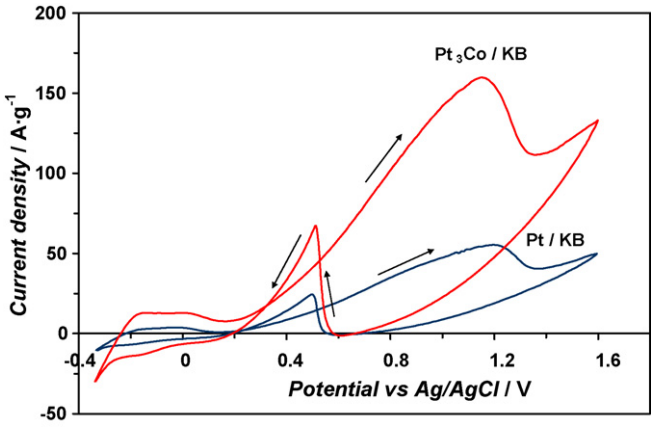

Fig. 8. Cyclic voltammograms of Pt/KB and Pt_3Co/KB catalyst electrodes in 0.5 mol dm^{-3} H_2SO_4 + 1 mol dm^{-3} methanol (25 °C, 20 mV s^{-1}); current normalised to the electrodes geometric area.

frequency arc decreases with decreasing cell voltage; for cell voltage higher than 0.4 V, the amplitude decreases with increasing air flow while, for cell voltage lower than 0.3 V, the amplitude is less and almost not affected by the air flow rate (Fig. 7b). The amplitude of the low frequency semicircle increases with the methanol concentration likely due to an increasing methanol crossover, and increases more for the Pt_3Co/KB cathode catalyst as expected from a less methanol tolerant catalyst.

It was also seen that the inductive loop related to methanol crossover disappears at low cell voltage. It is well known that methanol crossover in a DMFC decreases significantly with an increase of current density due to the decrease of methanol concentration gradient at the anode–electrolyte interface [1]. Under significant methanol crossover, a high flow rate of air is necessary to regenerate the catalyst sites [31] and this could explain the decrease in the amplitude of the semicircle with the flow rate for high cell voltage (higher crossover) and its independence at low cell voltage (lower crossover).

Although spectra fitting, quantification and interpretation are still under investigation, a comparison and qualitative interpretation of the present ac-impedance spectra have shown that the charge transfer resistance for the ORR occurring in the low frequency range dominates the overall DMFC impedance response. In addition it can be hypothesized that the impedance for the ORR in the presence of methanol is higher for the Pt_3Co/KB cathode catalyst due to a large effect of the mixed potential being the oxidation of the methanol permeated through the membrane faster on this catalyst.

Fig. 8 shows the cyclic voltammograms of both Pt/KB and Pt_3Co/KB catalysts based gas diffusion electrodes, recorded in nitrogen saturated 0.5 mol dm^{-3} H_2SO_4 + 0.5 mol dm^{-3} methanol solution. In the forward scan, the electrode coverage by CO-like residues strongly adsorbed on the surface occurs at low potentials, and these species are subsequently stripped off the surface only at high potentials [33]. The anodic peak occurring between 1.0 and 1.2 V vs. Ag/AgCl in the forward scan is related to the diffusion-controlled oxidation process of methanol to CO_2 [33]. At potentials of 1.5–1.6 V vs. Ag/AgCl, the oxygen evolution becomes prevailing and the electrode surface is covered by a strong oxide layer. The anodic peak occurring at about 0.5 V vs. Ag/AgCl in the reverse scan is also related to the methanol oxidation; however, it occurs on a Pt-oxide free surface after the PtO reduction to metallic Pt. In the reverse scan, and after the PtO reduction, a labile adsorption of OH species occurs on the surface and the coverage of methanolic species is smaller with respect to the forward scan since the electrode was previously covered by a strong oxide layer [33].

Fig. 8 shows that for the Pt_3Co/KB alloy catalyst the methanol oxidation peak in the forward and reverse scans are positioned at a significant lower potential with respect to the Pt/KB catalyst indicating that the Pt_3Co/KB has a much higher activity for methanol oxidation and therefore a lower methanol tolerance. In addition, the current density for methanol oxidation is significantly higher for the Pt_3Co/KB electrode due to the promoting effect of the electropositive element in adsorbing oxygen species necessary for the removal of the adsorbed methanolic residues.

The Pt-Co alloy catalysts are promising catalysts for the ORR in PEMFCs. The catalysts investigated in this work have already been examined for the ORR; the PtCo catalyst has shown superior performance than Pt and better resistance to degradation [24]. PtCo catalysts have been sometime proposed as methanol tolerant cathode catalyst based on dilution effect of Pt to decrease methanol chemisorption. Yet, the presence of electropositive elements (like Co) alloyed to Pt decreases the Pt 5 d-band vacancy [34]. An electron transfer from Co to Pt in a carbon-supported PtCo alloy has been reported in a previous paper [35]. As clearly evidenced by the present cyclic voltammetry results, no methanol oxidation occurs when Pt is covered by a strong oxide layer. Furthermore, the onset of methanol adsorption in the reverse scan occurs first (higher potentials) for the Pt_3Co alloy. This indicates that the reduction process of the oxide layer on the alloy catalyst is shifted to higher potentials. In fact, without the reduction of the oxide layer, no methanol oxidation may occur. Thus, Pt is less covered by strong oxide species on the Pt_3Co as previously observed by surface analysis studies [34]. The larger metallic character of Pt in the alloy catalyst favours the adsorption of methanolic species and the cleavage of the C—H bonds [1]. Besides, according to the bifunctional mechanism for methanol oxidation, the role of the second element in the Pt alloy is to promote OH adsorption on the catalyst surface at lower potentials favouring methanol oxidation [1]. In the literature, it has been observed that the addition of Co to Pt has two opposite effects [7], and the Co content in the alloy seems to determine which effect is preponderant: low Co content has a negative effect on the methanol oxidation (thus a positive effect on the methanol tolerance), instead high Co content increases the activity of the catalysts for methanol oxidation. However, a significant enhancement of oxygen reduction is observed for PtCo catalysts with suitable Co content and high degree of alloying [12,24].

The Pt_3Co/KB alloy catalyst used in this work, although promising for the ORR [24], is more active for methanol oxidation and thus less tolerant to methanol during the ORR, than the Pt catalyst prepared in the same way.

4. Conclusions

The performance of carbon-supported Pt and Pt_3Co cathode catalysts has been investigated in direct methanol fuel cells equipped with a conventional Nafion 117 membrane. The Pt_3Co catalyst shows better performance than a Pt catalyst of similar crystallite size and morphology only at low temperatures and in the presence of a low methanol concentration feed at the anode. Such conditions correspond to low methanol permeation through the membrane. This indicates poor methanol tolerance for this catalyst. This aspect is further confirmed by the cyclic voltammetry analysis, previous studies of the electronic properties of the Pt_3Co alloy as compared to Pt, and EIS experiments under different conditions. From ac-impedance, it is derived that the charge transfer resistance for the ORR dominates the overall DMFC impedance response. This effect is larger for the Pt_3Co/KB catalyst, indicating a lower methanol tolerance of this catalyst compared to Pt/KB. However, the development of methanol impermeable membranes could provide better chances of using PtCo catalyst as cathodes in DMFCs due to the promising activity towards oxygen reduction.

Acknowledgements

S. Siracusano acknowledges the Italian National Council of Research for the financial support of a short-term-mobility period at the Institut National de la Recherche Scientifique in Varennes (Québec, Canada). A.C. Tavares acknowledges the financial support from NSERC (Discovery Grant) and FQRNT (Nouveaux Chercheurs) agencies.

References

[1] A.S. Aricò, S. Srinivasan, V. Antonucci, Fuel Cells 1 (2001) 133.
[2] S.K. Kamarudin, W.R.W. Daud, S.L. Ho, U.A. Hasran, J. Power Sources 163 (2007) 743.
[3] A.K. Shukla, R.K. Raman, N.A. Choudhury, K.R. Priolkar, P.R. Sarode, S. Emura, R. Kumashiro, J. Electroanal. Chem. 563 (2004) 181.
[4] K. Scott, W. Yuan, H. Cheng, J. Appl. Electrochem. 37 (2007) 21.
[5] A. Stassi, C. D'Urso, V. Baglio, A. Di Blasi, V. Antonucci, A.S. Arico, A.M. Castro Luna, A. Bonesi, W.E. Triaca, J. Appl. Electrochem. 36 (2006) 1143.
[6] H. Yang, C. Coutanceau, J.-M. Leger, N. Alonso-Vante, C. Lamy, J. Electroanal. Chem. 576 (2005) 305.
[7] E. Antolini, J.R.C. Salgado, E.R. Gonzalez, Appl. Catal. B 63 (2006) 137.
[8] J.R.C. Salgado, E. Antolini, E.R. Gonzalez, Appl. Catal. B 57 (2005) 283.
[9] W. Li, W. Zhou, H. Li, Z. Zhou, B. Zhou, G. Sun, Q. Xin, Electrochim. Acta 49 (2004) 1045.
[10] M. Neergat, A.K. Shukla, K.S. Gandhi, J. Appl. Electrochem. 31 (2001) 373.
[11] H.A. Gasteiger, N.M. Markovic, P.N. Ross, E.J. Cairns, Electrochim. Acta 39 (1994) 1825.
[12] A.S. Aricò, A. Stassi, E. Modica, R. Ornelas, I. Gatto, E. Passalacqua, V. Antonucci, J. Power Sources 178 (2008) 525.
[13] R.C. Koffi, C. Coutanceau, E. Garnier, J.M. Leger, C. Lamy, Electrochim. Acta 50 (2005) 4117.
[14] U.A. Paulus, A. Wokaun, G.G. Scherer, T.J. Schmidt, V. Stamenkovic, V. Radmilovic, N.M. Markovic, P.N. Ross, J. Phys. Chem. B 106 (2002) 4181.
[15] A.M. Castro Luna, A. Bonesi, W.E. Triaca, V. Baglio, V. Antonucci, A.S. Aricò, J. Solid State Electrochem. 12 (2008) 643.
[16] A. Hamnett, Catal. Today 38 (1997) 445.
[17] S. Mukerjee, S. Srinivasan, J. Electroanal. Chem. 357 (1993) 201.
[18] E. Antolini, T. Lopes, E.R. Gonzalez, J. Alloy Compd. 461 (2008) 253.
[19] H.G. Petrow, R.J. Allen, US Patent 3, 992, 331 (1976).
[20] N. Giordano, E. Passalacqua, L. Pino, A.S. Aricò, V. Antonucci, M. Vivaldi, K. Kinoshita, Electrochim. Acta 36 (1991) 1979.
[21] A.S. Aricò, V. Baglio, A. Di Blasi, E. Modica, P.L. Antonucci, V. Antonucci, J. Electroanal. Chem. 557 (2003) 167.
[22] V. Baglio, A.S. Aricò, A. Stassi, C. D'Urso, A. Di Blasi, A.M. Castro Luna, V. Antonucci, J. Power Sources 159 (2006) 900.
[23] V. Baglio, A. Stassi, A. Di Blasi, C. D'Urso, V. Antonucci, A.S. Aricò, Electrochim. Acta 53 (2007) 1361.
[24] A. Stassi, E. Modica, V. Antonucci, A.S. Aricò, Fuel Cells, doi:10.1002/fuce.200800062, available on-line 20 January 2009.
[25] A.S. Aricò, A.K. Shukla, K.M. el-Khatib, P. Cretì, V. Antonucci, J. Appl. Electrochem. 29 (1999) 671.
[26] B.C. Beard, P.N. Ross, J. Electrochem. Soc. 137 (1990) 3368.
[27] L. Xiong, A. Manthriram, J. Mater. Chem. 14 (2004) 1454.
[28] M. Lucariello, N. Penazzi, E. Arca, G. Mulas, S. Enzo, Mater. Chem. Phys. 114 (2009) 227.
[29] H.A. Gasteiger, S.S. Kocha, B. Sompalli, F.T. Wagner, Appl. Catal. B 56 (2005) 9.
[30] J.T. Mueller, P.M. Urban, J. Power Sources 75 (1998) 139.
[31] P. Piela, R. Fields, P. Zelenay, J. Electrochem. Soc. 153 (2006) A1902.
[32] K. Furukawa, K. Okajima, M. Sudoh, J. Power Sources 139 (2005) 9.
[33] B.D. McNicol, D.A.J. Rand, K.R. Williams, J. Power Sources 83 (1999) 15.
[34] S. Mukerjee, S. Srinivasan, M.P. Soriaga, J. Electrochem. Soc. 142 (1995) 1409.
[35] A.S. Aricò, A.K. Shukla, H. Kim, S. Park, M. Min, V. Antonucci, Appl. Surf. Sci. 172 (2001) 33.